# Accepted Manuscript


Higher Naevus Count Exhibits A Distinct DNA Methylation Signature in Healthy Human Skin: Implications for Melanoma

Leonie Roos, Johanna K. Sandling, Christopher G. Bell, Daniel Glass, Massimo Mangino, Tim D. Spector, Panos Deloukas, Veronique Bataille, Jordana T. Bell

PII: S0022-202X(16)32787-7

DOI: 10.1016/j.jid.2016.11.029

Reference: JID 662

To appear in: *The Journal of Investigative Dermatology*

Received Date: 4 July 2016

Revised Date: 14 October 2016

Accepted Date: 21 November 2016

Please cite this article as: Roos L, Sandling JK, Bell CG, Glass D, Mangino M, Spector TD, Deloukas P, Bataille V, Bell JT, Higher Naevus Count Exhibits A Distinct DNA Methylation Signature in Healthy Human Skin: Implications for Melanoma, *The Journal of Investigative Dermatology* (2017), doi: 10.1016/j.jid.2016.11.029.

# HIGHER NAEVUS COUNT EXHIBITS A DISTINCT DNA METHYLATION SIGNATURE IN HEALTHY HUMAN SKIN: IMPLICATIONS FOR MELANOMA

Leonie Roos[1], Johanna K. Sandling[2], Christopher G Bell[1,3-5], Daniel Glass[1], Massimo Mangino[1], Tim D Spector[1], Panos Deloukas[6], Veronique Bataille[1*], and Jordana T Bell*[1]

* Joint contribution

**Affiliations**

[1] Department of Twin Research and Genetic Epidemiology, King's College London, London SE1 7EH, UK;

[2] Department of Medical Sciences, Molecular Medicine and Science for Life Laboratory, Uppsala University, 751 85 Uppsala, Sweden;

[3] MRC Lifecourse Epidemiology Unit, University of Southampton, Southampton SO16 6YD, UK;

[4] Human Development and Health Academic Unit, Institute of Developmental Sciences, University of Southampton, Southampton SO16 6YD, UK;

[5] Epigenomic Medicine, Centre for Biological Sciences, Faculty of Environmental and Natural Sciences, University of Southampton, Southampton SO17 1BJ, UK;

[6] William Harvey Research Institute, Queen Mary University of London, London EC1M 6BQ, UK.

Corresponding author:

Leonie Roos; leonie.roos@kcl.ac.uk, phone: + 44 (0)20 718 81508

**ABSTRACT**

High naevus count is the strongest risk factor for melanoma and although gene variants have been discovered for both traits, epigenetic variation is unexplored. We investigated 322 healthy human skin DNA methylomes associated with total body naevi count, incorporating genetic and transcriptomic variation.

DNA methylation changes were identified at genes involved in melanocyte biology, such as *RAF1* ($p$ = 1.2 x $10^{-6}$) and *CTC1* (region: $p$ = 6.3 x $10^{-4}$), and other genes including *ARRDC1* ($p$ = 3.1 x $10^{-7}$). A subset exhibited coordinated methylation and transcription changes within the same biopsy. The total analysis was also enriched for melanoma-associated DNA methylation variation ($p$ = 6.33 x $10^{-6}$). Additionally, we show that skin DNA methylation is associated in *cis* with known GWAS SNPs for naevus count, at *PLA2G6* ($p$ = 1.7 x $10^{-49}$) and *NID1* ($p$ = 6.4 x $10^{-14}$), as well as melanoma risk, including in or near *MC1R*, *MX2* and *TERT*/*CLPTM1L* ($p < 1 \times 10^{-10}$).

Our analysis using a uniquely large dataset comprising healthy skin DNA methylomes identified known and additional regulatory loci and pathways in naevi and melanoma biology. This integrative study improves our understanding of predisposition to naevi and their potential contribution to melanoma pathogenesis.

## INTRODUCTION

The total body number of melanocytic naevi is the strongest risk and predictive factor for melanoma in Caucasian populations (Gandini et al. 2005; Olsen et al. 2009). Melanoma is the most aggressive of skin tumours with an increasing incidence (Siegel et al. 2014). These malignancies arise from an existing benign naevus in 20% to 50% of cases (Haenssle HA et al. 2016; Purdue et al. 2005; Shitara et al. 2014; Weatherhead et al. 2007). The vast majority of naevi never progress to melanoma, however naevi count is still a predisposition marker for melanoma arising de novo (Chang et al. 2009). Therefore, further understanding of the biology of naevi will give insights into the development and pathology of melanoma.

Typically, the number of naevi decrease after the age of 40, however, in individuals at high risk of melanoma, this loss of naevi is delayed, reflecting an altered senescence (Newton et al. 1993). Furthermore, a higher total body naevus count has also been associated with longer telomere length in blood in individuals from the TwinsUK cohort (Bataille et al. 2007). This link with senescence may indicate that the total numbers of naevi reflect differences in senescence pathways between individuals that can be detected in skin tissue where naevi are found. The usefulness of naevus counts as an intermediate phenotype to melanoma has already been shown in genome-wide association studies (GWAS), as common single nucleotide polymorphisms (SNPs) in the loci *PLA2G6* and *MTAP* were first associated with total body naevus count (Falchi et al. 2009; Nan et al. 2011) and then subsequently with melanoma risk (Barrett et al. 2011; Bishop et al. 2009). For naevus count, variants in *PLA2G6* were replicated across two studies that also identified additional associations in *NID1, c11orf74,* and *MTAP*. Though GWAS have identified genetic variation for naevi count and melanoma, the variance in naevus counts

explained by these genes is low and no study has previously examined epigenetic variation in this context.

Here, we explore epigenome-wide DNA methylation variation in healthy human skin tissue in relation to total body naevus counts in 322 female individuals from the TwinsUK cohort. The focus of this study is on the potential to identify a predisposing DNA methylation signature of normal skin to the number of naevi and not the malignant changes occurring in melanocytes themselves. It has become increasingly acknowledged that cross talk between all cells within the skin and melanocytes is important in the progression to melanoma (Kaur et al. 2016; Kim et al. 2013; Li et al. 2003; Shih et al. 1994). We investigated individual CpG differentially methylated positions (DMPs), as well as differentially methylated regions (DMRs) in healthy skin tissue, and corresponding gene expression changes within the same tissue. To study the potential interaction between genetic variants and DNA methylation, we examined the association between the skin DNA methylome and genetic variants previously associated with naevus count or melanoma risk by GWAS.

## RESULTS

### The skin DNA methylome and its tissue layer specificity

As expected, due to the differing cell types in skin within the dermis and epidermis, these tissue layers harbour distinct DNA methylation profiles (Vandiver et al. 2015). In our study, skin tissue DNA was derived from a peri-umbilical punch biopsy (adipose tissue was removed from the biopsy before freezing) from 322 healthy female twins and profiled using the Infinium HumanMethylation450 BeadChip. To confirm which skin layer was represented in our biopsy sample, we compared our DNA methylation dataset to recently published DNA methylation profiles of mechanically separated epidermal (36 individuals) and dermal tissue (36 individuals) from Vandiver *et al.* (Vandiver et al. 2015). Principal component analysis (PCA) was performed on unadjusted DNA methylation profiles of the three groups of samples (dermis (n=40), epidermis (n=38), and our whole skin sample (n=322)). The first two principal components (PCs) explain 55.6% of the variance, capturing the skin layer specificity of the dermis and epidermis samples as previously shown (Vandiver et al. 2015). Our whole skin DNA methylation profiles cluster closely with the dermal layer DNA methylation profiles (Figure 1).

### Single CpG site differential skin DNA methylation in relation to total body naevus count

We first explored evidence for differential skin DNA methylation associated with total body naevus count at the single CpG-site level across the genome in 322

healthy female twins. We fitted a linear mixed effects model regressing DNA methylation levels on fixed effects (age, BMI, smoking status, chip, order on the chip, and bisulphite conversion efficiency) and random effects (family structure and zygosity). Three differentially methylated positions were identified to be significantly associated with total body naevus count (n-DMPs) at a false discovery rate (FDR) of 5% and a further 45 associations were observed at a FDR of 10% (Figure 2 A, Table 1, Table S1). The 48 n-DMPs are enriched for strong enhancers (ChromHMM state 4) in the NHEK cell line derived from epidermal keratinocytes ($p$ = 0.03) and for CpG island (CGI) shores (2kb either side of the CGI, $p$ = 0.04), while depleted for signals located in open sea genomic regions that are more than 4kb beyond CGIs ($p$ = 2.2 x $10^{-3}$).

The strongest signals are shown Table 1 and Figure 2 B. The most associated signal (cg06244240, $p$ = 5.5 x $10^{-8}$) lies in a CGI shore ~6.5kb downstream of *METRNL*, which is expressed in skin (Ushach et al. 2015) and is also involved in neural cell formation. The second ranked signal (cg06123942, $p$ = 2.2 x $10^{-7}$) is in the 5' CGI promoter of *C15orf48*, that displays reduced expression in squamous cell carcinoma (Freiberger et al. 2015). The third ranked signal (cg25384157, $p$ = 3.1 x $10^{-7}$) is positively associated with the number of naevi and is in a CGI shore ~1.5kb upstream of the transcription start site (TSS) of *ARRDC1*, a negative regulator of the Notch signalling pathway (Puca et al. 2013). The CpG (cg11297934, $p$ = 1.2 x $10^{-6}$) lies ~200 bp upstream of the TSS of proto-oncogene *RAF1* (also known as *CRAF)*, which is a member of the RAF family in the ERK/MAPK pathway that includes the key player *BRAF*.

Six out of our top 10 n-DMPs did not show direct association with age ($p$ = 0.05) including two of the top four results (*ARRDC1* and *RAF1)*, with no n-DMP

associations with age surpassing FDR 10% correction (Figure 2 C). The remaining four signals did not show stronger evidence for association with age alone compared to naevus count. These results suggest that the majority of top-ranked n-DMPs are not directly associated with age.

**Regional differential skin DNA methylation associated with total body naevus count**

We next aimed to identify differentially methylated regions, that is, small genomic regions that contain multiple CpG sites and show consistent directional association with total body naevus count (n-DMRs). DMRs have been found in general to be enriched for functionally relevant regions as well as for GWAS SNPs from the GWAS catalogue (Ziller et al. 2013). We applied the BumpHunter (Jaffe et al. 2012) algorithm and identified 48 n-DMRs ($p < 0.01$) genome-wide (Table 2, Table S2).

Subsequently, we examined the genomic context of the n-DMRs. The strongest signal ($p = 6.8 \times 10^{-5}$, Figure 3 A) was observed overlapping the 5' CGI promoter of *ARRDC1*. This n-DMR includes the third ranked FDR 5% individual CpG n-DMP (cg25384157). We also identified an n-DMR in *CTC1* that shows consistent negative association with total body naevus count amongst its three CpG sites (Figure 3 B). It is in a region with active promoter evidence across multiple ENCODE cell types including NHEK, that resides in the 3' UTR of *CTC1* but also 2kb upstream of the lincRNA *LINC00324*. *CTC1* is a component of the CTS complex that has a pivotal role in protecting telomeres from degradation.

**Naevus differential methylation signatures reflected in gene expression changes**

We then explored individual CpG sites in the 48 n-DMRs for association with gene expression levels using transcription profiles available in 248 individuals using the same skin biopsy as for DNA methylation profiling. The analysis focused on CpG sites that showed the same direction of effect in the n-DMR as in the single CpG site EWAS. We analysed gene expression data at 36 genes for 27 n-DMRs, where the n-DMRs were either located in or were within 20kb of the gene (Table S3). Both DNA methylation and expression levels were adjusted for similar covariates and corresponding technical covariates and compared with Pearson correlation. At least one CpG site in 12 unique n-DMRs were shown to be correlated with the expression levels of 14 unique genes at nominal significance ($p$ = 0.05, Table S3). This included one of the three CpG sites forming the third ranked n-DMR in *KCNN4* (cg15977816, r = 0.19, $p$ = 2.9 x $10^{-3}$). Strong n-DMRs that have more than one CpG site in the region correlated with one of more expression probes of the same gene include n-DMRs at: *MED11*, *C14orf50*, *FAM64A*, *KRT86*, *TTC15*, and *C6orf27*.

**Naevus DNA methylation signature is enriched for melanoma associated DNA methylation changes**

Healthy tissue DNA methylomes can show risk-factor related signatures also found in malignant tissue (Noreen et al. 2014). Furthermore, tumour methylation patterns have been shown to derive from the continuum of maturation states that are reflected in normal developmental stages (Oakes et al. 2016). We therefore examined the DNA methylome data of melanomas to see whether our identified n-DMP signature was enriched within this malignant tissue epigenome.

The most comprehensive melanoma DNA methylome study to date is a comparison between normal melanocytes from three donors and 27 metastatic

melanoma DNA samples using methylated-CpG island recovery assay sequencing (MIRA-Seq) by Jin *et al*. (Jin et al. 2015). They reported 3,113 regions that were hypermethylated in melanoma. Of these, 2,039 regions contained at least one CpG site profiled in our dataset and 13.4% (274 regions, containing 406 CpG sites) of these were identified as nominally significant with a positive association to total body naevus count. Within CGIs, which the MIRA-Seq technique targets, we observed an enrichment of hypermethylated nominally significant CpG sites (Fisher's $p = 6.33 \times 10^{-6}$). Another study, a genome-wide screen of promoter DNA methylation (24,103 RefSeq promoters) between normal skin, naevi, and advanced stage melanoma identified four differentially methylated genes (Koga et al. 2009). At two of these genes, *THBS1* and *TNFRSF10D*, we identified a positive association between total body naevus count and promoter CpG methylation, in line with their findings of increased DNA methylation in advanced stage melanoma.

**Impact of GWAS SNPs associated with total body naevus count or melanoma risk on skin DNA methylation in *cis***

We next investigated the influence of genetic variants, previously associated in GWAS with naevus count or melanoma risk, on nearby DNA methylation levels in skin tissue for a subset of 283 individuals. We selected 4 SNPs previously associated with the number of cutaneous naevi (Falchi et al. 2009; Nan et al. 2011) and 23 SNPs associated with melanoma risk from the GWAS catalogue (Welter et al. 2014) that fall within 100 kb of CpG sites available in our dataset. Mixed linear models were performed to test for association accounting for family structure and results are presented at a threshold of $p < 1.0 \times 10^{-5}$. This is comparable to a genomewide cut-off

at FDR 1%, as reported previously ($p < 8.6 \times 10^{-4}$) where all DNA methylation was assessed within 100 kb of common genetic variants (Grundberg et al. 2013).

Thirteen SNPs were significantly associated with DNA methylation changes in skin ($p < 1 \times 10^{-5}$, Table 3). These included three of the four SNPs identified by GWAS to be associated with total body naevus count: rs2284063 in intron of *PLA2G6* (cg25457927, $p = 3.5 \times 10^{-38}$), rs3768080 in intron of *NID1* (cg18765906, $p = 6.4 \times 10^{-14}$), and rs738322 in another intron of *PLA2G6* (cg25457927, $p = 1.7 \times 10^{-49}$). The results also included ten SNPs previously identified for melanoma risk reported at *MC1R* (2 SNPs), *MX2*, *TERT*/*CLPTM1L*, *PLA2G6*, *CASP8*, *ACTRT3*, *ASIP*, *CDC91L1*, and *ARNT/SETDB1/LASS2ANXA9/MCL1/CTSK* (Figure 4). Six of these CpG sites occurred in active promoters or enhancers in NHEK (derived from epidermal keratinocytes) (Ernst et al. 2011). None of the CpG sites associated with these SNPs were epigenome-wide statistically significant n-DMPs or within n-DMRs from our EWAS analysis. However, 9 naevus count CpG sites within these regions were associated with naevus count at nominally significance ($p = 0.05$), including the result at *PLA2G6*.

The thirteen SNPs have not been previously reported as expression quantitative loci (eQTL) using the same skin biopsy expression data (Grundberg et al. 2012). However, results from the Genotype-Tissue Expression Project (GTEx) (Consortium 2015) datasets show that eight of these SNPs are eQTLs in either skin tissue (sun or not sun exposed) and/or transformed fibroblasts. These GTEx eQTLs were associated with the expression of 16 genes in total, and at seven of these we identified DNA methylation variation associated with the same SNP: *CASP8* (rs1301693), *MAFF*, *PLA2G6*, *TMEM184B*, and *BAIAP2L2* (rs2284063, rs738322, and rs6001027), *SPATA33* (rs258322), *MX2* (rs45430), and *CDK10* (rs4785763).

## DISCUSSION

To our knowledge, this is the first study to explore epigenome-wide DNA methylation in the largest healthy human skin tissue dataset to date, in relation to number of naevi, the strongest risk factor of melanoma. This analysis adds an additional layer to our current understanding of the genomic biology of naevi development on top of that previously obtained via GWAS. We used normal skin biopsies of 322 healthy female twins and showed that these biopsies represent mostly homogenous dermis cells due to their distinct epigenetic signature. We identified DNA methylation variation associated with total body naevus count at, to our knowledge, previously unreported genes and also at known genes in naevi formation or melanoma, both at single CpGs as well as regions. These top-ranked results are significantly enriched for strong enhancers in NHEK cell lines as well as for CGI shores, regions identified as more dynamic and functional in both cancer (Irizarry et al. 2009) and stem cell reprogramming (Doi et al. 2009). Approximately half of the regional epigenetic changes tested also had corresponding gene expression differences in the same biopsy. Finally, we identified DNA methylation variation in *cis* associated with known GWAS SNPs for both naevi number and melanoma risk

We identified many genomic loci that exhibited differential methylation associated with total body naevus count that were highly relevant to melanocyte biology and cancer. Among these is the n-DMR at *CTC1*, involved in telomere maintenance and associated with telomere length (Mangino et al. 2012). Telomere length has been positively associated with high naevus count and melanoma risk (Bataille et al. 2007), as well as via a genetic score analysis from 7 telomere length associated SNPs (Iles et al. 2014). This suggests that telomeres within healthy skin

may already be longer in high naevus count individuals as a similar rate of age-dependent telomere length attrition has been shown between leukocytes and skin (Daniali et al. 2013), and supports previous work in melanoma biology . It may also explain why individuals with multiple atypical naevi are relatively protected against photo ageing, due to potential reduced skin senescence.

An important molecular pathway highlighted, due to differential DNA methylation in *RAF1,* is the MAP/ERK pathway that includes *BRAF*. *BRAF* mutations are found in ~50% of all melanoma tumours and are of significant clinical utility as major therapeutic decisions are made according to the presence or absence of mutations in this gene (Flaherty et al. 2010). Somatic mutations in the oncogene *RAF1* are remarkably rare in human cancers (Emuss et al. 2005), however, in *BRAF* negative melanomas, targeting *RAF1* leads to apoptosis. Therefore the significant identification that this pathway is altered via DNA methylation could lead to the re-evaluation of using mutational status alone in advanced melanoma treatment decisions (Heyn and Esteller 2012).

Another result of note is *ARRDC1,* part of the highly conserved cell signalling NOTCH pathway. This pathway is pivotal in cell-fate determination across many organ systems in embryogenesis and also tissue maintenance in adults. Expression of *Notch1* is low or not detectable in melanocytes as well as naevi, however, higher expression is associated with their transformation to melanoma (Massi et al. 2006; Pinnix et al. 2009). *ARRDC1* is necessary for Itch E3 ubiquitin ligase mediated NOTCH receptor degradation (Puca et al. 2013).

We also found that our naevi signature was enriched for DNA methylation changes previously identified in melanoma (Jin et al. 2015). This may indicate a priming or predisposition to melanoma of normal skin with more naevi. We then

investigated the effect of 26 unique genetic variants, previously associated by GWAS with naevus number (4 SNPs) or melanoma risk (23 SNPs), on DNA methylation within 100 kb (Falchi et al. 2009; Nan et al. 2011; Welter et al. 2014). Half of these SNPs were significantly associated with DNA methylation changes in skin tissue. For all three GWAS SNPs reported for *PLA2G6,* which is associated with both naevus numbers and melanoma, eQTLs have been reported in skin and/or transformed fibroblasts impacting on the expression of *PLA2G6, MAFF, TMEM184B,* and *BAIAP2L2.* All of these genes harboured SNP-associated DNA methylation variation in our study. This highlights the usefulness of integrating DNA methylation analysis with robust GWAS discoveries to identify functional pathways underlying strong genetic signals. Furthermore, we identified GWAS SNP-associated DNA methylation variation, not only in genes with known eQTLs, but also in novel genes.

Compared to other studies, our sample is much larger than previous skin DNA methylation studies (Roberson et al. 2012; Rodríguez et al. 2014; Vandiver et al. 2015), and we have profiled only women, who are known to have different distribution of naevi on the body compared to men (Autier et al. 2004) as well as sex-specific differences in DNA methylation (Singmann et al. 2015). Additionally, this study benefits from the extensive data for naevus counts collected by trained dermatology nurses of healthy individuals. In contrast to blood-based EWAS, this study also highlights the strength of investigating the phenotype-appropriate tissue to help understand biological pathways implicated in disease.

To conclude, this study based on skin biopsies of 322 healthy female Caucasians using DNA methylome, transcriptome, and GWAS data from the same individuals identified DNA methylation differences associated with number of naevi. We identified pathways and genes that add to our current understanding of the

biology of the number of naevi and the pathology of melanoma. These data open up avenues for future exploration in skin, not only why some individuals have higher numbers of naevi but how this phenotype contributes to melanoma risk.

## MATERIALS AND METHODS

### Sample selection

Detailed information regarding naevus count was obtained from twins registered with the TwinsUK Adult Twin Registry. The twins in this registry are not selected for diseases and were similar in means and ranges of quantitative phenotypes to an age-matched population in the UK (Andrew et al. 2001). Written informed consent from all subjects was obtained in accordance with Guy's & St Thomas' NHS Foundation Trust Ethics Committee (EC04/015 - 15-Mar-04). The selected individuals did not have a personal medical history of malignant melanoma or other skin cancers obtained through record linkage with the National Cancer Registry at the Office for National Statistics (ONS). The examination was performed by trained research nurses following a standardised and reproducible naevus count protocol as described previously (Bataille et al. 2000). Total body naevus count was the sum of all naevi > 2mm across 17 body sites.

DNA methylation data profiled from skin tissue was available for 322 female twins with a mean age of 59 years old, including 25 MZ twin-pairs, 64 DZ twin-pairs, and 144 unrelated individuals of European descent. Punch biopsies (8 mm) were taken from a relatively photo-protected area adjacent and inferior to the umbilicus and were mechanically dissected for skin tissue removing the fat layer prior to freezing. Written informed consent from all study subjects was obtained and the procedures were in accordance with the ethical standards of the St. Thomas' Research Ethics Committee (REC reference 07/H0802/84). The skin biopsy samples were obtained within 6.5 and 11.9 years after naevus count with a mean of 9.7 years (Figure S1).

**Genome-wide DNA methylation profiles**

Genome-wide DNA methylation profiles were obtained from 326 bisulphite-converted skin tissue DNA samples assayed by Illumina Infinium HumanMethylation450 BeadChip. DNA methylation levels were denoted as betas: the ratio of intensity signal from the methylated probes over the sum of intensity signals from both unmethylated and methylated probes. Multiple measurements of analytical quality were applied. Probes were removed for the main analyses that: failed detection in at least one sample or had a bead count less than 3 in more than 1% of the samples (n=18,208), had a 50 bp probe sequence that aligned to multiple locations in the genome (n=17,764), harboured common genetic variants (MAF $\geq$ 1%) within 10 bp on the probe at the interrogated CpG site (15,827), or contained variants at any MAF within 10 bp at the interrogated CpG site (11,236), and were located on the sex chromosomes (n=11,650). Probes with genetic variants within the 50 bp of the CpG, but not within 10 bp were not excluded for GWAS SNP analyses but were highlighted as such in the figures and accompanying text.

Individuals were verified using the 57 autosomal SNP probes included as control probes on the BeadChip. Overall intensity signal as well as bisulphite conversion efficiency were assessed and the data was inspected visually for outliers using beta density plots, boxplots, and imprinted regions (using the R package wateRmelon (Schalkwyk et al. 2013)). Four individual samples were excluded based on low mean intensity signals. The remaining 322 samples were normalised using the BMIQ method to correct for probe type bias (Teschendorff et al. 2013). Principal component analysis (PCA) was performed on BMIQ normalised beta values that were standardised (N(0,1)) at each probe. The first three principle components (PCs), which when combined explain 36% of the total variance, were assessed for

associations with possible confounders for DNA methylation data including BeadChip, position on the BeadChip, age, smoking status, body mass index (BMI), and bisulphite conversion efficiency. Strongly significant associations ($p < 1 \times 10^{-20}$) were identified with BeadChip and bisulphite conversion efficiency.

**Gene expression profiles**

Gene expression profiles were obtained of the same skin tissue biopsies which were profiled for DNA methylation for 248 individuals from the MuTHER project (Multiple Tissue Human Expression Resource) as previously described (Grundberg et al. 2012). In short, punch biopsies (8mm) were taken from a photo-protected area adjacent and inferior to the umbilicus of which skin tissue was dissected. RNA was extracted and expression profiling was performed using Illumina Human HT-12 V3 BeadChips. Probes with less than three beads present were excluded and $\log_2$-transformed expression signals were normalized separately per tissue, with quantile normalization of the replicates of each individual followed by quantile normalization across all individuals.

**Genotypes**

Genotype data of 283 individuals were available from the TwinsUK dataset as previously described (Small et al. 2011), genotyped using a combination of Illumina HumanHap300, HumanHap610Q, 1M-Duo, or 1.2M-Duo custom arrays. Imputation was done based on 1000 Genomes data phase 3. Quality control measures included minimum genotyping rate (>95 %), Hardy–Weinberg equilibrium ($p > 10^{-6}$), minimum MAF (>1%) and imputation quality score >0.5 for GWAS catalogue SNPs. This subset of individuals included only individuals of Caucasian ancestry.

**Statistical analysis**

DMPs associated with total body naevus count were identified using a linear mixed effects model fitted on the normalized beta values per probe (N(0,1)) with total body naevus count, age, BMI, smoking, bead chip, position on the bead chip, and bisulphite conversion efficiency as fixed effects, and family and zygosity as random effects. This model was compared to a null model that excluded total body naevus count by ANOVA. Results were considered genome-wide significant if they surpassed a FDR threshold of 5% and considered suggestive when surpassing an FDR of 10%, estimated using 'qvalue' in R.

Naevus count DMPs were tested for association with age using a linear mixed effects model fitted on the normalized beta values per probe (N(0,1)) with age, BMI, smoking status, BeadChip, position on the BeadChip, and bisulphite conversion efficiency as fixed effects, and family and zygosity as random effects. This was compared to a null model without age by ANOVA to test for significance.

Small differentially methylated regions (DMRs) associated with naevus count were identified using R package 'Bumphunter' (Jaffe et al. 2012). Regions required at least three consecutive probes with a maximum gap of 500 bp between each probe. DNA methylation was adjusted for covariates described previously for DMP analysis before using Bumphunter. Naevus count DMRs were considered with a p-value < 0.01 estimated based on 1000 permutations.

Gene expression analysis of the top-ranked DMRs was performed in a sample of 248 individuals using the same skin tissue biopsy used for DNA methylation profiling. A linear mixed model was fitted on the expression data with age, BMI, smoking status, batch, and concentration (fixed effects) and family and zygosity (random effects) as well as the linear mixed model fitted for DNA methylation data

described previously for n-DMP analysis. The residuals from both models were compared with Pearson correlation.

Genotype variation analyses using GWAS SNPs were performed in a sample of 283 individuals using genome-wide efficient mixed model association (GEMMA) to account for family structure present in the data and adjusted DNA methylation levels for fixed covariates used in the n-DMP analysis (age, BMI, smoking status, BeadChip, position on the BeadChip, and bisulphite conversion efficiency).

## CONFLICT OF INTEREST

The authors declare that there is no conflict of interest.

## ACKNOWLEDGEMENTS

This work was supported by EU-FP7 project EpiTrain (316758). TwinsUK received funding from the Wellcome Trust; European Community's Seventh Framework Programme (FP7/2007-2013), the National Institute for Health Research (NIHR)-funded BioResource, Clinical Research Facility and Biomedical Research Centre based at Guy's and St Thomas' NHS Foundation Trust in partnership with King's College London. SNP Genotyping was performed by The Wellcome Trust Sanger Institute and National Eye Institute via NIH/CIDR. JKS was supported by a Swedish Research Council postdoc grant (Dnr 350-2012-256).

## AVAILABLITY OF DATA AND MATERIALS

The DNA methylation data of the 322 individuals for this article are in the Gene Expression Omnibus (GEO) with accession code GSE90124.

## REFERENCES

Andrew T, Hart DJ, Snieder H, de Lange M, Spector TD, MacGregor AJ. Are Twins and Singletons Comparable? A Study of Disease-related and Lifestyle Characteristics in Adult Women. Twin Res. Hum. Genet. 2001 Dec;4(6):464–477.

Autier P, Boniol M, Severi G, Pedeux R, Grivegnée A-R, Doré J-F, et al. Sex Differences in Numbers of Nevi on Body Sites of Young European Children: Implications for the Etiology of Cutaneous Melanoma. Cancer Epidemiol. Biomarkers Prev. 2004 Dec 1;13(12):2003–5.

Barrett JH, Iles MM, Harland M, Taylor JC, Aitken JF, Andresen PA, et al. Genome-wide association study identifies three new melanoma susceptibility loci. Nat. Genet. 2011 Nov;43(11):1108–13.

Bataille V, Kato BS, Falchi M, Gardner J, Kimura M, Lens M, et al. Nevus Size and Number Are Associated with Telomere Length and Represent Potential Markers of a Decreased Senescence In vivo. Cancer Epidemiol. Biomarkers Prev. 2007 Jul 1;16(7):1499–502.

Bataille V, Snieder H, MacGregor AJ, Sasieni P, Spector TD. Genetics of risk factors for melanoma: an adult twin study of nevi and freckles. J. Natl. Cancer Inst. 2000 Mar 15;92(6):457–63.

Bishop DT, Demenais F, Iles MM, Harland M, Taylor JC, Corda E, et al. Genome-wide association study identifies three loci associated with melanoma risk. Nat. Genet. 2009 Aug;41(8):920–5.

Chang Y, Newton-Bishop JA, Bishop DT, Armstrong BK, Bataille V, Bergman W, et al. A pooled analysis of melanocytic nevus phenotype and the risk of cutaneous melanoma at different latitudes. Int. J. Cancer. 2009 Jan 15;124(2):420–8.

Consortium TGte. The Genotype-Tissue Expression (GTEx) pilot analysis: Multitissue gene regulation in humans. Science. 2015 May 8;348(6235):648–60.

Daniali L, Benetos A, Susser E, Kark JD, Labat C, Kimura M, et al. Telomeres shorten at equivalent rates in somatic tissues of adults. Nat. Commun. 2013 Mar 19;4:1597.

Doi A, Park I-H, Wen B, Murakami P, Aryee MJ, Irizarry R, et al. Differential methylation of tissue- and cancer-specific CpG island shores distinguishes human induced pluripotent stem cells, embryonic stem cells and fibroblasts. Nat. Genet. 2009 Dec 1;41(12):1350–3.

Emuss V, Garnett M, Mason C, Project TCG, Marais R. Mutations of C-RAF Are Rare in Human Cancer because C-RAF Has a Low Basal Kinase Activity Compared with B-RAF. Cancer Res. 2005 Nov 1;65(21):9719–26.

Ernst J, Kheradpour P, Mikkelsen TS, Shoresh N, Ward LD, Epstein CB, et al. Systematic analysis of chromatin state dynamics in nine human cell types. Nature. 2011 May 5;473(7345):43–9.

Falchi M, Bataille V, Hayward NK, Duffy DL, Bishop JAN, Pastinen T, et al. Genome-wide association study identifies variants at 9p21 and 22q13 associated with development of cutaneous nevi. Nat. Genet. 2009 Aug 1;41(8):915–9.

Flaherty KT, Hodi FS, Bastian BC. Mutation-driven drug development in melanoma. Curr. Opin. Oncol. 2010 May;22(3):178.

Freiberger SN, Cheng PF, Iotzova-Weiss G, Neu J, Liu Q, Dziunycz P, et al. Ingenol Mebutate Signals via PKC/MEK/ERK in Keratinocytes and Induces Interleukin Decoy Receptors IL1R2 and IL13RA2. Mol. Cancer Ther. 2015 Sep 1;14(9):2132–42.

Gandini S, Sera F, Cattaruzza MS, Pasquini P, Abeni D, Boyle P, et al. Meta-analysis of risk factors for cutaneous melanoma: I. Common and atypical naevi. Eur. J. Cancer. 2005 Jan;41(1):28–44.

Grundberg E, Meduri E, Sandling JK, Hedman AK, Keildson S, Buil A, et al. Global analysis of DNA methylation variation in adipose tissue from twins reveals links to disease-associated variants in distal regulatory elements. Am. J. Hum. Genet. 2013 Nov 7;93(5):876–90.

Grundberg E, Small KS, Hedman ÅK, Nica AC, Buil A, Keildson S, et al. Mapping cis- and trans-regulatory effects across multiple tissues in twins. Nat. Genet. 2012 Oct;44(10):1084–9.

Haenssle HA, Mograby N, Ngassa A, et al. ASsociation of patient risk factors and frequency of nevus-associated cutaneous melanomas. JAMA Dermatol. 2016 Mar 1;152(3):291–8.

Heyn H, Esteller M. DNA methylation profiling in the clinic: applications and challenges. Nat. Rev. Genet. 2012 Oct;13(10):679–92.

Iles MM, Bishop DT, Taylor JC, Hayward NK, Brossard M, Cust AE, et al. The effect on melanoma risk of genes previously associated with telomere length. J. Natl. Cancer Inst. 2014 Oct;106(10).

Irizarry RA, Ladd-Acosta C, Wen B, Wu Z, Montano C, Onyango P, et al. The human colon cancer methylome shows similar hypo- and hypermethylation at conserved tissue-specific CpG island shores. Nat. Genet. 2009 Feb 1;41(2):178–86.

Jaffe AE, Murakami P, Lee H, Leek JT, Fallin MD, Feinberg AP, et al. Bump hunting to identify differentially methylated regions in epigenetic epidemiology studies. Int. J. Epidemiol. 2012 Feb 1;41(1):200–9.

Jin S-G, Xiong W, Wu X, Yang L, Pfeifer GP. The DNA methylation landscape of human melanoma. Genomics. 2015 Dec;106(6):322–30.

Kaur A, Webster MR, Marchbank K, Behera R, Ndoye A, Kugel CH, et al. sFRP2 in the aged microenvironment drives melanoma metastasis and therapy resistance. Nature. 2016 Apr 14;532(7598):250–4.

Kim E, Rebecca V, Fedorenko IV, Messina JL, Mathew R, Maria-Engler SS, et al. Senescent fibroblasts in melanoma initiation and progression: an integrated theoretical, experimental, and clinical approach. Cancer Res. 2013 Dec 1;73(23):6874–85.

Koga Y, Pelizzola M, Cheng E, Krauthammer M, Sznol M, Ariyan S, et al. Genome-wide screen of promoter methylation identifies novel markers in melanoma. Genome Res. 2009 Aug;19(8):1462–70.

Li G, Satyamoorthy K, Meier F, Berking C, Bogenrieder T, Herlyn M. Function and regulation of melanoma–stromal fibroblast interactions: when seeds meet soil. Oncogene. 2003;22(20):3162–71.

Mangino M, Hwang S-J, Spector TD, Hunt SC, Kimura M, Fitzpatrick AL, et al. Genome-wide meta-analysis points to CTC1 and ZNF676 as genes regulating telomere homeostasis in humans. Hum. Mol. Genet. 2012 Dec 15;21(24):5385–94.

Massi D, Tarantini F, Franchi A, Paglierani M, Serio CD, Pellerito S, et al. Evidence for differential expression of Notch receptors and their ligands in melanocytic nevi and cutaneous malignant melanoma. Mod. Pathol. 2006 Feb 1;19(2):246–54.

Nan H, Xu M, Zhang J, Zhang M, Kraft P, Qureshi AA, et al. Genome-wide association study identifies nidogen 1 (NID1) as a susceptibility locus to cutaneous nevi and melanoma risk. Hum. Mol. Genet. 2011 Apr 9;ddr154.

Newton JA, Bataille V, Griffiths K, Squire JM, Sasieni P, Cuzick J, et al. How common is the atypical mole syndrome phenotype in apparently sporadic melanoma? J. Am. Acad. Dermatol. 1993 Dec 1;29(6):989–96.

Noreen F, Röösli M, Gaj P, Pietrzak J, Weis S, Urfer P, et al. Modulation of Age- and Cancer-Associated DNA Methylation Change in the Healthy Colon by Aspirin and Lifestyle. J. Natl. Cancer Inst. 2014 Jul 1;106(7):dju161.

Oakes CC, Seifert M, Assenov Y, Gu L, Przekopowitz M, Ruppert AS, et al. DNA methylation dynamics during B cell maturation underlie a continuum of disease phenotypes in chronic lymphocytic leukemia. Nat. Genet. 2016 Mar 1;48(3):253–64.

Olsen CM, Zens MS, Stukel TA, Sacerdote C, Chang Y-M, Armstrong BK, et al. Nevus density and melanoma risk in women: A pooled analysis to test the divergent pathway hypothesis. Int. J. Cancer. 2009 Feb 15;124(4):937–44.

Pinnix CC, Lee JT, Liu Z-J, McDaid R, Balint K, Beverly LJ, et al. Active Notch1 Confers a Transformed Phenotype to Primary Human Melanocytes. Cancer Res. 2009 Jul 1;69(13):5312.

Puca L, Chastagner P, Meas-Yedid V, Israël A, Brou C. α-arrestin 1 (ARRDC1) and β-arrestins cooperate to mediate Notch degradation in mammals. J Cell Sci. 2013 Oct 1;126(19):4457–68.

Purdue MP, From L, Armstrong BK, Kricker A, Gallagher RP, McLaughlin JR, et al. Etiologic and Other Factors Predicting Nevus-Associated Cutaneous Malignant Melanoma. Cancer Epidemiol. Biomarkers Prev. 2005 Aug 1;14(8):2015–22.

Roberson EDO, Liu Y, Ryan C, Joyce CE, Duan S, Cao L, et al. A subset of methylated CpG sites differentiate psoriatic from normal skin. J. Invest. Dermatol. 2012 Mar;132(3 0 1):583–92.

Rodríguez E, Baurecht H, Wahn AF, Kretschmer A, Hotze M, Zeilinger S, et al. An Integrated Epigenetic and Transcriptomic Analysis Reveals Distinct Tissue-Specific Patterns of DNA Methylation Associated with Atopic Dermatitis. J. Invest. Dermatol. 2014 Jul;134(7):1873–83.

Schalkwyk LC, Pidsley R, Wong CC, Touleimat N, Defrance M, Teschendorff A, et al. wateRmelon: Illumina 450 methylation array normalization and metrics. 2013.

Shih IM, Elder DE, Hsu MY, Herlyn M. Regulation of Mel-CAM/MUC18 expression on melanocytes of different stages of tumor progression by normal keratinocytes. Am. J. Pathol. 1994 Oct;145(4):837–45.

Shitara D, Nascimento MM, Puig S, Yamada S, Enokihara MMSS, Michalany N, et al. Nevus-Associated Melanomas. Am. J. Clin. Pathol. 2014 Oct 1;142(4):485–91.

Siegel R, Ma J, Zou Z, Jemal A. Cancer statistics, 2014. CA. Cancer J. Clin. 2014 Jan 1;64(1):9–29.

Singmann P, Shem-Tov D, Wahl S, Grallert H, Fiorito G, Shin S-Y, et al. Characterization of whole-genome autosomal differences of DNA methylation between men and women. Epigenetics Chromatin. 2015 Oct 19;8(1):1.

Small KS, Hedman AK, Grundberg E, Nica AC, Thorleifsson G, Kong A, et al. Identification of an imprinted master trans regulator at the KLF14 locus related to multiple metabolic phenotypes. Nat. Genet. 2011 Jun;43(6):561–4.

Teschendorff AE, Marabita F, Lechner M, Bartlett T, Tegner J, Gomez-Cabrero D, et al. A beta-mixture quantile normalization method for correcting probe design bias in Illumina Infinium 450 k DNA methylation data. Bioinforma. Oxf. Engl. 2013 Jan 15;29(2):189–96.

Ushach I, Burkhardt AM, Martinez C, Hevezi PA, Gerber PA, Buhren BA, et al. METEORIN-LIKE is a cytokine associated with barrier tissues and alternatively activated macrophages. Clin. Immunol. 2015 Feb;156(2):119–27.

Vandiver AR, Irizarry RA, Hansen KD, Garza LA, Runarsson A, Li X, et al. Age and sun exposure-related widespread genomic blocks of hypomethylation in nonmalignant skin. Genome Biol. 2015 Apr 16;16(1):80.

Weatherhead SC, Haniffa M, Lawrence CM. Melanomas arising from naevi and de novo melanomas — does origin matter? Br. J. Dermatol. 2007 Jan 1;156(1):72–6.

Welter D, MacArthur J, Morales J, Burdett T, Hall P, Junkins H, et al. The NHGRI GWAS Catalog, a curated resource of SNP-trait associations. Nucleic Acids Res. 2014 Jan 1;42(D1):D1001–6.

Ziller MJ, Gu H, Müller F, Donaghey J, Tsai LT-Y, Kohlbacher O, et al. Charting a dynamic DNA methylation landscape of the human genome. Nature. 2013 Aug 22;500(7463):477–81.

Table 1. Most associated naevus differential methylation positions (nDMPs)

| **Rank** | **CpG** | **Position (hg19)** | **Associated gene** | **Location** | **CpG island** | **Beta** | **St. Error** | ***P* value** | **FDR** |
|---|---|---|---|---|---|---|---|---|---|
| 1 | cg06244240 | chr17: 81058948 | - | - | Shore | 0.0052 | 0.0009 | $5.52 \times 10^{-8}$ | 5% |
| 2 | cg06123942 | chr15: 45722795 | *C15orf48* | 5'UTR | Island | -0.0074 | 0.0014 | $2.20 \times 10^{-7}$ | 5% |
| 3 | cg25384157 | chr9: 140499131 | *ARRDC1* | TSS1500 | Shore | 0.0063 | 0.0012 | $3.06 \times 10^{-7}$ | 5% |
| 4 | cg11297934 | chr3:12705868 | *RAF1* | TSS200 | Island | -0.0046 | 0.0009 | $1.16 \times 10^{-6}$ | 10% |
| 5 | cg14762973 | chr2:187714067 | *ZSWIM2* | TSS200 | Island | 0.0069 | 0.0014 | $1.49 \times 10^{-6}$ | 10% |

Table 2. Most associated naevus differential methylation regions (nDMRs)

| **Rank** | **Position (hg 19)** | **Associated Gene** | **Location** | **CpG Island** | **Number of CpG sites** | **DNA methylation** | ***P* value** | **Overview direction CpG sites** |
|---|---|---|---|---|---|---|---|---|
| 1 | chr9:140499132-140500813 | *ARRDC1* | TSS1500-Body | Island | 7 | + | $2.5 \times 10^{-5}$ | + + - - - + + |
| 2 | chr10:14647154-14647530 | *FAM107B* | Body | Shore | 3 | + | $2.5 \times 10^{-4}$ | + + + |
| 3 | chr19:44285297-44285568 | *KCNN4* | TSS200-1stExon | - | 3 | + | $2.9 \times 10^{-4}$ | + + + |
| 4 | chr17:8129997-8130356 | *CTC1* | 3'UTR | Shelf | 3 | - | $6.3 \times 10^{-4}$ | - - - |
| 5 | chr15:26915414-26915752 | *GABRB3* | Body | Island | 3 | - | $8.3 \times 10^{-4}$ | - - - |

Table 3. Strongest CpG association per GWAS SNP.

| **Trait** | **rs** | **Position (hg19)** | **Reported Genes** | **cpg** | **beta** | **P value** | **Associated Gene** | **Location** | **CpG Island** | **Distance to SNP (kb)** |
|---|---|---|---|---|---|---|---|---|---|---|
| Melanoma | rs401681 | chr5:1322087 | *TERT, CLPTM1L* | cg06550200 | 0.783 | $2.6 \times 10^{-50}$ | CLPTM1L | Body | - | -3.5 |
| Cutaneous nevi | rs738322 | chr22:38569006 | *PLA2G6* | cg25457927 | 0.851 | $1.7 \times 10^{-49}$ | - | - | Shelf | -26.4 |
| Melanoma | rs45430 | chr21:42746081 | *MX2* | cg22778903 | -0.711 | $1.9 \times 10^{-42}$ | MX2 | 5'UTR | - | 4.4 |
| Melanoma | rs6001027 | chr22:38545619 | *PLA2G6* | cg25457927 | 0.843 | $1.3 \times 10^{-38}$ | - | - | Shelf | -49.8 |
| Cutaneous nevi & Melanoma | rs2284063 | chr22:38544298 | *PLA2G6* | cg25457927 | 0.834 | $3.5 \times 10^{-38}$ | - | - | Shelf | -51.1 |
| Melanoma | rs7412746 | chr1:150860471 | *ARNT, SETDB1, LASS2, ANXA9,* | cg15448220 | 0.662 | $1.4 \times 10^{-32}$ | SETDB1 | TSS1500 | Shore | -37.4 |

| | | | | | | | | | | |
|---|---|---|---|---|---|---|---|---|---|---|
| | | | *MCL1, CTSK* | | | | | | | |
| Melanoma (2) | rs258322 | chr16:89755903 | *MC1R* | cg05714116 | -0.728 | $5.5 \times 10^{-14}$ | CDK10 | TSS1500 | Shore | 3.3 |
| Cutaneous nevi | rs3768080 | chr1:236179869 | *NID1* | cg18765906 | -0.374 | $6.4 \times 10^{-14}$ | NID1 | Body | - | 4.5 |
| Melanoma | rs4785763 | chr16:90066936 | *MC1R* | cg08547343 | -0.346 | $1.0 \times 10^{-9}$ | CENPBD1; AFG3L1 | 5'UTR; TSS200 | Island | 28.1 |
| Melanoma | rs910873 | chr20:33171772 | *CDC91L1* | cg01901788 | -0.441 | $1.8 \times 10^{-6}$ | MAP1LC3A | TSS1500 | Shore | 25.9 |
| Melanoma | rs13097028 | chr3:169464942 | *ACTRT3* | cg27020690 | -0.289 | $2.0 \times 10^{-6}$ | - | - | Island | -17.4 |
| Melanoma | rs13016963 | chr2:202162811 | *CASP8* | cg24599065 | -0.230 | $2.1 \times 10^{-6}$ | CASP10 | 3'UTR | - | 69.0 |
| Melanoma | rs228437 | chr6:134898456 | *ASIP* | cg24504307 | -0.355 | $9.2 \times 10^{-6}$ | - | - | - | -64.7 |
| Melanoma | rs3219090 | chr1:226564691 | *PARP1* | cg18764804 | 0.240 | $6.2 \times 10^{-4}$ | PARP1 | TSS1500 | Shore | -32.0 |
| Melanoma | rs1031925 | chr3:51379274 | *DOCK3* | cg09456445 | -0.315 | $8.5 \times 10^{-4}$ | DOCK3 | 3'UTR | Shore | -41.1 |
| Melanoma | rs1722784 | chr1:150961869 | *ANXA9* | cg07479786 | 0.261 | $8.9 \times 10^{-4}$ | ANXA9 | 3'UTR | - | -6.0 |
| Melanoma | rs1695300 | chr16:54114824 | *FTO* | cg01083598 | -0.169 | $7.2 \times 10^{-3}$ | - | - | Island | -41.2 |

| | | | | | | | | | | |
|---|---|---|---|---|---|---|---|---|---|---|
| | 2 | | | | | | | | | |
| Melanoma | rs35390 | chr5:33955326 | *SLC45A2* | cg01990593 | 0.689 | $8.8 \times 10^{-3}$ | ADAMTS12 | Body | Shore | 65.0 |
| Melanoma | rs1801516 | chr11:108175462 | *ATM* | cg08954307 | -0.249 | $9.8 \times 10^{-3}$ | ATM | Body | - | -59.3 |
| Cutaneous nevi | rs4636294 | chr9:21747803 | *MTAP* | cg03724238 | -0.128 | 0.013 | - | - | Island | 51.1 |
| Melanoma | rs4698934 | chr4:106139387 | *TET2* | cg08530497 | -0.195 | 0.037 | TET2 | Body | - | -15.9 |
| Melanoma | rs1847134 | chr11:89005253 | *TYR* | cg25941151 | -0.153 | 0.041 | TYR | TSS200 | - | 94.3 |
| Melanoma (2) | rs7023329 | chr9:21816528 | *CDKN2A* | cg14548963 | 0.118 | 0.068 | MTAP | Body | - | 3.6 |
| Melanoma (2) | rs1393350 | chr11:89011046 | *TYR* | cg03508346 | -0.118 | 0.142 | NOX4 | 3'UTR | - | -48.8 |
| Melanoma | rs17119461 | chr10:107516352 | *NR* | cg18758405 | -0.290 | 0.333 | - | - | - | 65.0 |
| Melanoma | rs1889497 | chr6:65432283 | *EYS* | cg11999886 | -0.026 | 0.760 | EYS | Body | - | 90.8 |

## FIGURE LEGENDS

**Figure 1. Global DNA methylation profiles and skin tissue specificity.**

First two principal components coloured by layer specificity; red for dermal tissue, blue for epidermal tissue, and green for our data (see legend)**.**

**Figure 2. Naevus count epigenome-wide results in 322 female individuals.**

**[a]** Manhattan plot of the epigenome-wide association results in 322 female individuals, where each point represents the observed $-\log_{10} p$ value at a CpG-site. **[b]** Panel plot depicting direction of association at the three top-ranked signals for cg06244240 (left), cg06123942 (middle), and cg25384157 (right). Results are plotted using normalised unadjusted beta values per individual. The lines represent the linear correlation between DNA methylation and total body naevus count. **[c]** Heatmap of top 48 ranked n-DMPs coloured by –log10 *p* values of age association and naevus association.

**Figure 3. Location of two top ranked n-DMRs in the human genome.**

Figures obtained from UCSC Genome browser, displaying position in the genome (hg19), CpG sites from HumanMethylation450 BeadChip, n-DMR (in light blue), RefSeq genes, CpG island, transcription factor ChIP data, DNase-I sensitivity sites, and ChromHMM genomic segmentation. **[a]** At *ARRDC1*. **[b]** At *CTC1*.

**Figure 4. GWAS SNPs for naevus count or melanoma risk vs DNA methylation in skin tissue in *cis*.**

Regional plot of 100kb flanking regions around the GWAS SNP of interest denoted as striped black line. Each point is a CpG site with its *p* value on the y-axis. The plots are annotated with a gene track from LocusZoom. Each point is coloured according to occurrence of genetic variants on the probe sequence (see legend) **[A]** rs738322 identified for cutaneous naevi **[B]** rs3768080 identified for cutaneous naevi **[C]** rs45430 identified for melanoma risk **[D]** rs401681 identified for melanoma risk.

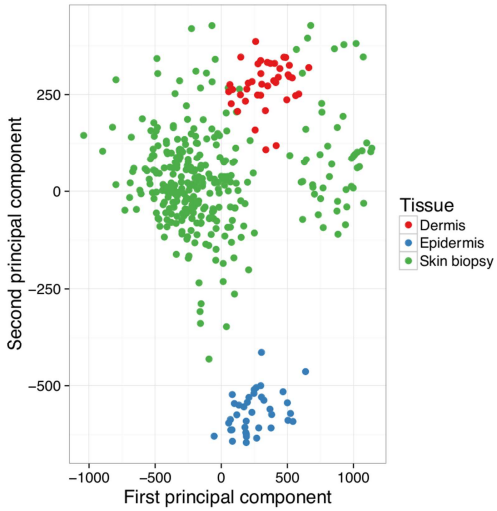

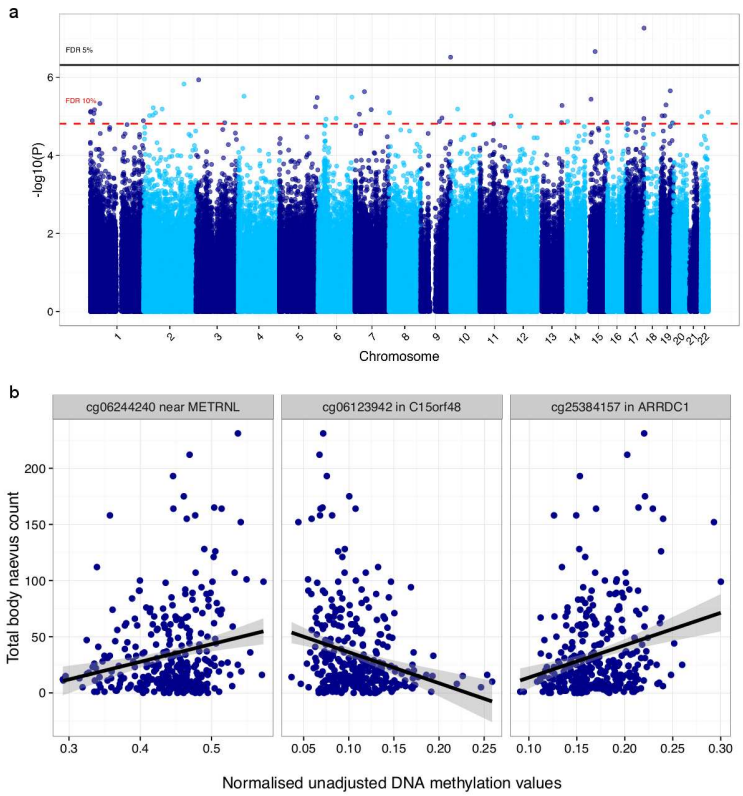
a
FDR 5%
FDR 10%
-log10(P)
Chromosome
b
cg06244240 near METRNL
cg06123942 in C15orf48
cg25384157 in ARRDC1
Total body naevus count
Normalised unadjusted DNA methylation values
c
Color Key
−log10 p value
Age
Naevus

a

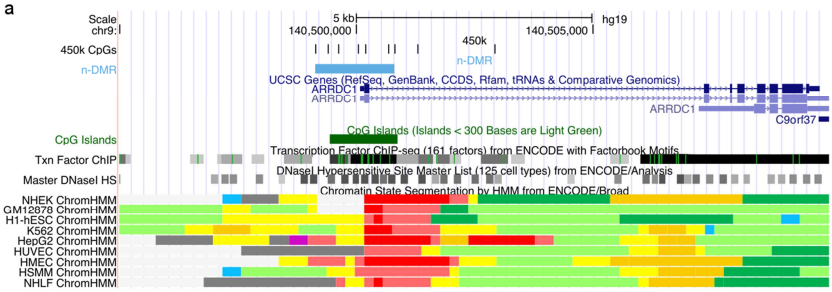


b